

31 December, 1997

Cross Section Measurements of Hard Diffraction at the $Spp\bar{S}$ -Collider

A. Brandt^{1a}, S. Erhan^b, A. Kuzucu², M. Medinnis³,
N. Ozdes², P.E. Schlein, M.T. Zeyrek⁴, J.G. Zweizig⁵
University of California*, Los Angeles, California 90024, USA.

J.B. Cheze, J. Zsembery
Centre d'Etudes Nucleaires-Saclay, 91191 Gif-sur-Yvette, France.

(UA8 Collaboration)

Abstract

The UA8 experiment previously reported the observation of jets in diffractive events containing leading protons (“hard diffraction”), which was interpreted as evidence for the partonic structure of an exchanged Reggeon, believed to be the \mathcal{P} omeron. In the present Letter, we report the final UA8 hard-diffractive (jet) cross section results and their interpretation. After corrections, the fraction of single diffractive events with mass from 118 to 189 GeV that have two scattered partons, each with $E_T^{jet} > 8$ GeV, is in the range 0.002 to 0.003 (depending on x_p). We determine the product, fK , of the fraction by which the \mathcal{P} omeron’s momentum sum rule is violated and the normalization constant of the \mathcal{P} omeron-Flux-Factor of the proton. For a pure gluonic- or a pure $q\bar{q}$ - \mathcal{P} omeron, respectively: $fK = (0.30 \pm 0.05 \pm 0.09)$ and $(0.56 \pm 0.09 \pm 0.17)$ GeV⁻².

Submitted to Physics Letters B

* Supported by U.S. National Science Foundation Grant PHY94-23142

^a email: brandta@fnalv.fnal.gov

^b email: samim.erhan@cern.ch

¹ Now at Fermi National Accelerator Laboratory, Batavia, Illinois, U.S.A.

² Visitor from Cukurova University, Adana, Turkey; also supported by ICSC - World Lab.

³ Present address: DESY, Zeuthen, Germany

⁴ Visitor from Middle East Tech. Univ., Ankara, Turkey; supported by Tubitak.

⁵ Present address: DESY, Hamburg, Germany

1 Introduction

During the last decade, the physics of \mathcal{P} omeron-exchange or diffractive (leading proton) processes,

$$\bar{p} + p_i \rightarrow X + p_f \quad + \text{charge conjugate}, \quad (1)$$

$$e^\mp + p_i \rightarrow e^\mp + X + p_f, \quad (2)$$

has taken a new direction:

- Ingelman and Schlein[1] proposed that the partonic structure of the exchanged Reggeons in Reactions 1 and 2 (dominated by the \mathcal{P} omeron[2]) could be studied if hard-scattering effects were observed in the interactions of the exchanged Reggeon with the \bar{p} in the first process and with a photon in the second. Based on the assumption of factorization, a method of analysis was proposed to extract the \mathcal{P} omeron structure function.
- This experiment, UA8 at the CERN collider ($\sqrt{s} = 630$ GeV), presented the first evidence[3] that the \mathcal{P} omeron has a partonic structure, with the observation of QCD jet production in React. 1. The observed event rate had the predicted[1] order of magnitude from \mathcal{P} omeron phenomenology. In a second Letter[4], which reported a sample of 300 2-jet events with $E_T^{jet} > 8$ GeV, an analysis of the longitudinal momentum distribution of the 2-jet system in the \mathcal{P} omeron-proton frame showed that the \mathcal{P} omeron internal structure is “hard”, like $x(1-x)^1$, with about 30% of the sample exhibiting a δ -function-like structure near $x = 1$. Furthermore, the fraction of diffractive events which exhibit hard scattering was observed to be independent of momentum-transfer, $|t|$, over the range 0.8-2.0 GeV².
- The ZEUS[5] and H1[6] experiments at HERA have observed related Deep-Inelastic hard-diffraction events in React. 2. They also find evidence for a hard \mathcal{P} omeron structure but, in addition, are able to demonstrate that there is a large gluonic component. In particular, H1 has recently presented[7] a QCD analysis of their data, from which they conclude that gluons carry 80–90% of the \mathcal{P} omeron’s momentum and that, at small- Q^2 , there is a parton concentration near $x = 1$ in the \mathcal{P} omeron system. This observation may be intimately related to the “super-hard” \mathcal{P} omeron structure reported by us in Ref. [4].

The DØ collaboration has confirmed the existence of hard diffraction in $p\bar{p}$ interactions at $\sqrt{s} = 630$ GeV and also report its existence at $\sqrt{s} = 1800$ GeV[8]. At 1800 GeV, the CDF collaboration has also obtained evidence that the \mathcal{P} omeron is dominantly gluonic, by comparing the measured rates of diffractive W-boson[9] and dijet[10] production.

Since the UA8 jet analyses probed the structure of the $\xi = 1 - x_p$ component of the proton, *independent of any assumptions about its identity*, it is important to study the jet cross section within the context of \mathcal{P} omeron phenomology. In this Letter, we report

the final UA8 hard diffractive (jet) cross section results and their interpretation. We extract new parameters from the data which can be used to predict other hard-diffraction cross sections, thus allowing tests of factorization and other aspects of hard diffraction phenomenology.

Preliminary results from these analyses were presented[11] at the 1993 Marseille Conference. Since then, much work has been done to further understand the phenomenology of single diffraction and the \mathcal{P} omeron-Flux-Factor, which is necessary for a more thorough understanding of the data. In particular, a detailed analysis[12] of our UA8 data, together with the data from other experiments has been performed. Some of the relevant results are discussed below.

We attempt to clarify several items. One key issue is to what extent the \mathcal{P} omeron behaves like a real particle, in the sense that the momentum fractions of its partons sum to unity (the “momentum sum rule”)[13, 14]. Another has to do with the (arbitrary) conventions used for the normalization of the \mathcal{P} omeron-Flux-Factor in the proton, an overall scale for the process, for which at least three versions exist in the literature[13, 14, 15].

2 Diffractive Jet Data sample

The momentum of the final state proton in Reaction 1, p_f , was measured in one of four small-angle UA8 “Roman-pot” spectrometers[16] which were interfaced to the UA2 experiment[17]; the final-state jets were measured in the upgraded UA2 calorimeter system. The inclusive proton data sample was provided by the so-called “DIF” trigger, whose data-acquisition logic required a proton or antiproton with an acceptable momentum that was calculated online[16, 18]. A second trigger, used to provide the jet event sample and denoted “JET”, combined the DIF trigger with the additional requirement that the total transverse energy in the UA2 calorimeter system had $\Sigma E_T > 18$ GeV (this cut was increased to 22 GeV in the offline analysis).

In Reaction 1, the incident \bar{p} interacts with a residual component of the incident proton, p_i , with beam momentum fraction¹, $\xi = 1 - x_p$, where $x_p = p_f/p_i$. The system X in Reaction 1 has squared invariant mass, $s' = s\xi$, so that in this experiment, for example, $\sqrt{s'} = 118$ (200) GeV when $\xi = 0.035$ (0.10).

Figure 1 shows our observed inclusive proton x_p distribution for both triggers. For the DIF trigger, the most likely value of x_p is near unity and, correspondingly, the most likely value of ξ is near zero. On the same plot, the solid points are those DIF-trigger events which satisfy the offline requirement, $\Sigma E_T > 18$ GeV. The lower histogram which is normalized to the solid points corresponds to the high-statistics sample for which the same ΣE_T selection was imposed online in the JET trigger. The ΣE_T selection discriminates against x_p values near 1.0, which are incapable of producing large s' values.

Figure 2 compares the uncorrected momentum-transfer distributions of data samples from the two triggers, with $0.90 < x_p < 0.97$ and with offline pileup and halo cleanup cuts

¹Because $x_p + \xi = 1$, we may refer to one or the other of these equivalent variables in this Letter.

imposed[19]. We conclude that, to good approximation, large- ΣE_T and low- ΣE_T events of React. 1 have the same t -dependence (in our region of t).

Jet-finding was performed using UA2 calorimeter cell information, by requiring that at least 8 GeV of transverse energy was deposited within a cone of unit radius (in $\eta - \phi$) around the direction of an initiator cell. Figure 3 shows a display of a typical 2-jet event. In this event, a recoil proton with $x_p \simeq 0.94$ has carried away much of the initial state energy, leaving an effective interaction energy $\sqrt{s'} \simeq 150$ GeV. The jets are clearly defined, with little underlying event background, and are separated by about 180° in azimuthal angle, as expected for the hard scattering of two partons (83% of the 2-jet events have $\Delta\phi > 135^\circ$). The shapes and other characteristics of the jets were shown[3, 4] to agree with QCD Monte-Carlo predictions. Table 1 lists the numbers of 2-jet events in four bins of x_p , where the jets satisfy a fiducial cut, $|\eta| < 2$, a coplanarity cut, $\Delta\phi > 135^\circ$ and are in a restricted t -range, 1.15-2.0 GeV².

We find that the fraction of triggered events with $\Sigma E_T > 22$ GeV that contain jets is the same at low- t and high- t in our data. The fraction is (0.384 ± 0.010) for $0.9 < t < 1.4$ GeV² and (0.376 ± 0.010) for $1.7 < t < 2.3$ GeV². Taking into account the observation that a ΣE_T selection itself does not alter the t -dependence, we conclude that *the t -dependence of React. 1 is the same with jets as without jets over our t -range*. We take this as a working assumption for the analysis presented in this Letter and note that is consistent with the hypothesis of factorization.

We define the parameter, \mathcal{R} , in a given $\Delta\xi$ bin in React. 1, as the fraction of the total single diffractive cross section that exhibits hard scattering. Not only is the \mathcal{R} ratio independent of t within our t -range, but the acceptance corrections for protons or antiprotons as well as certain systematic uncertainties cancel.

$$\mathcal{R} = \frac{\Delta\sigma_{sd}^{jets}}{\Delta\sigma_{sd}^{total}} = \frac{N_j/(\mathcal{L}_j\epsilon_j A_j)}{N_{sd}/(\mathcal{L}_{sd}\epsilon_{sd})} = \frac{N_j}{N_{sd}} \cdot \frac{1}{A_j} \cdot \frac{\mathcal{L}_{sd}}{\mathcal{L}_j} \cdot \frac{\epsilon_{sd}}{\epsilon_j} \quad (3)$$

N_j and N_{sd} are the numbers of diffractive jet events and inclusive single diffractive events, respectively (the 1989 data sample used in the present analysis had a luminosity for the sample of jet events of $\mathcal{L}_j = 423$ nb⁻¹). The efficiencies, $\epsilon_j = 0.50$ and $\epsilon_{sd} = 0.83$, correct for good events which are lost in the offline rejection of pileup and halo events[12, 16, 19]. A_j is the jet acceptance[19] for the events in the numerator and, for a hard gluonic Pomeron, is 0.44 at $x_p = 0.91$, decreasing to 0.19 at $x_p = 0.965$. A_j is 20% larger for a hard $q\bar{q}$ Pomeron.

A_j was calculated with a modified version of the PYTHIA 4.8 event generator[20, 21], in which the Pomeron is defined as a beam particle, with gluonic or $q\bar{q}$ structure, and a proton is the target particle². Hard Pomeron-proton interactions at a specific $\sqrt{s'}$ are calculated for any assumed Pomeron structure function, using standard QCD parton-parton scattering matrix elements with initial and final state radiation. In PYTHIA, the minimum transverse momentum of the parton-parton hard scattering, QTMIN, was set

²We have since used POMPYT 2.6, which is based on PYTHIA 5.7, to verify that our Pomeron structure conclusions are unaffected by changing to the most recent proton structure functions.

to 1/2 the desired jet threshold of 8 GeV, in order to maximize the fraction of generated events that are useful for the analysis without biasing the jet distribution.

JETSET 6.3[22] was used to model the hadronization according to the Lund string model[23]. The generated Monte Carlo events were then boosted from the \mathcal{P} omeron-proton system to the laboratory frame where they were passed through the UA2 calorimeter simulation[24]. Finally, the simulated event sample was passed through pattern recognition, jet-finding and selection software, identical to that used in the processing of real data.

This procedure allows us to relate the number of events with two $E_T^{jet} > 8$ GeV jets, to the events generated with scattered partons with $p_T > 8$ GeV. Defining A_j as the ratio of these numbers, we follow a convention where the *scattered parton cross section* is quoted as the “jet cross section”, thus facilitating comparison with theoretical predictions.

Equation 3 is evaluated for diffractive mass bins from 118 to 189 GeV and the resulting values of \mathcal{R} are given in Table 1. \mathcal{R} is evaluated for both a hard gluonic and a hard $q\bar{q}$ \mathcal{P} omeron, differing only in the A_j value used, and is found to be in the range 0.0017 to 0.0028. The absolute jet cross sections are given below.

The dominant source of the systematic uncertainty in \mathcal{R} (26%) is the jet acceptance calculation, to which three sources contribute equally and are combined in quadrature: uncertainties in “tuning” PYTHIA to describe the underlying events, the choice of the proton structure function and the choice of the minimum transverse momentum of the parton-parton scattering. Imperfect agreement of the jet-finding yield between Monte-Carlo and data, when the cone size and initiator energy of the jet-finding algorithm are changed, leads to an “Algorithm” error (10%). The estimated uncertainty (10%) on the ratio of the efficiency parameters is dominated by the correction for pileup-rejected events (superimposed diffractive event with a minimum-bias event) that contain a diffractive event which alone has ΣE_T above the trigger threshold. These components are added in quadrature to give a total 30%.

We note one point concerning the “super-hard” component in the data[4]. These events, whose 2-jet longitudinal momentum component in the \mathcal{P} omeron-proton center-of-mass is larger than 0.7, constitute about 30% of the entire 2-jet sample. Although the super-hard events are included in the N_j of Table 1, the component is not explicitly included in the calculation of A_j . Since the jet-acceptance is about 20% larger for these events than for the hard structure function used in the calculation of A_j , the total effect on the values of \mathcal{R} of Table 1 is $\sim 6\%$. However, we ignore this, because our systematic uncertainty is 30%.

3 Phenomenology

We assume factorization, as in Ref. [1], such that the observed hard-scattering cross section in React. 1 is a product of the \mathcal{P} omeron-Flux-Factor[13], $F_{\mathcal{P}/p}(t, \xi)$, and the cross section for \mathcal{P} omeron-proton hard scattering.

The QCD hard scattering takes place between a parton in the \mathcal{P} omeron and a parton

in the proton or antiproton and is calculated by POMPYT 2.6 with default settings:

$$f \cdot \sigma_{\mathcal{P}p}^{jets} = \int dx_1 dx_2 d\hat{t} \sum_{i,k} g(x_1) G_i(x_2, Q^2) \frac{d\hat{\sigma}_i^k}{d\hat{t}}. \quad (4)$$

$\sigma_{\mathcal{P}p}^{jets}$ is the hard scattering cross section if the momentum sum rule is valid for the Pomeron. x_1 is the momentum fraction of a parton in the Pomeron with effective structure $xg(x) = f \cdot 6x(1-x)^1$, where $f \neq 1.0$ denotes a violation of the momentum sum rule. x_2 is the momentum fraction of a parton in a proton with CTEQ2L structure function, $G_i(x_2, Q^2)$. The cross section is based on the standard QCD matrix elements, $d\hat{\sigma}_i^k/d\hat{t}$, and the summations go over all possible parton-parton scattering subprocesses. The scale, Q^2 , of the proton structure is equated to $(E_T^{jet})^2$ and Q^2 evolution of the Pomeron structure function is ignored, because it is believed to be small in our E_T^{jet} -range, as is any possible dependence on t . The leading order values³ of $\sigma_{\mathcal{P}p}^{jets}$ for hard gluon and hard quark structures, are given in Table 1.

In the ξ -range in which non-Pomeron-exchange background is small enough to be ignored (see below for a discussion of this point), the hard-scattering and the total single diffractive single-arm cross sections in React. 1 can be written as:

$$\frac{d^2 \sigma_{sd}^{jets}}{d\xi dt} = F_{\mathcal{P}/p}(t, \xi) \cdot [f \cdot \sigma_{\mathcal{P}p}^{jets}(s')] \quad (5)$$

$$\frac{d^2 \sigma_{sd}^{total}}{d\xi dt} = F_{\mathcal{P}/p}(t, \xi) \cdot \sigma_{\mathcal{P}p}^{total}(s'), \quad (6)$$

The ratio of Eqs. 5 and 6 gives us, on the left-hand side, the measured t -independent \mathcal{R} parameter defined in Sec. 2. The Flux-Factor cancels out on the right-hand side and we have Eq. 2 of Ref. [1]:

$$\mathcal{R}(s') = \frac{\Delta \sigma_{sd}^{jets}}{\Delta \sigma_{sd}^{total}} = f \cdot \frac{\sigma_{\mathcal{P}p}^{jets}(s')}{\sigma_{\mathcal{P}p}^{total}(s')}. \quad (7)$$

Previously[3], we used the simple assumption, $f = 1$. We also assumed a constant $\sigma_{\mathcal{P}p}^{total} = 2.3$ mb, based on triple-Regge analyses[25, 26, 27, 14] of single diffractive data. Now, however, we wish to determine f from experiment and allow $\sigma_{\mathcal{P}p}^{total}$ to have a proper Regge dependence on s' . Our current analysis is carried out with the following steps:

- From Eq. 7, it is seen that the measurements of \mathcal{R} (*appropriately background corrected*) and calculations of $\sigma_{\mathcal{P}p}^{jets}(s')$ in Table 1 permit the determination of the ratio, $f/\sigma_{\mathcal{P}p}^{total}(s')$.
- Fitting Eq. 6 to inclusive single diffractive data permits the Pomeron-proton total cross section, $\sigma_{\mathcal{P}p}^{total}(s')$, as well as parameters of the Pomeron flux factor, $F_{\mathcal{P}/p}(t, \xi)$, to be determined. This step of the analysis is made using much higher statistics, and data at different energies, which is necessary to determine $F_{\mathcal{P}/p}(t, \xi)$. Theoretical uncertainty in the value of the overall normalization constant, K , in $F_{\mathcal{P}/p}(t, \xi)$ means that only the product $K\sigma_{\mathcal{P}p}^{total}(s')$ can be uniquely determined.

³If we include NLO contributions, using an effective k factor, the cross sections increase by 20-30%.

- The product of $f/\sigma_{\mathcal{P}p}^{total}(s')$ and $K\sigma_{\mathcal{P}p}^{total}(s')$ yields the quantity, fK , which can be directly used to make predictions with Eq. 5 (providing $F_{\mathcal{P}/p}(t, \xi)$ is known). Furthermore, the simplest factorization assumptions imply that fK should be independent of both s' and s (see Sec. 4 for a further discussion of this point).

In a separate article[12], our collaboration has reported a complete analysis of inclusive single diffraction. Combined fits of Eq. 6 were made to UA8 and lower energy ISR data[28] ($s = 551$ and 930 GeV²) in the momentum transfer range, $0.15 < t < 2.0$ GeV² with the following forms of $F_{\mathcal{P}/p}(t, \xi)$ and $\sigma_{\mathcal{P}p}^{total}(s')$:

$$\frac{d^2\sigma_{sd}^{total}}{d\xi dt} = F_{\mathcal{P}/p}(t, \xi) \cdot \sigma_{\mathcal{P}p}^{total}(s') = [K F_1(t)^2 e^{bt} \xi^{1-2\alpha(t)}] \cdot \sigma_0[(s')^{0.10} + R(s')^{-0.32}] \quad (8)$$

$F_1(t)^2$ is the standard Donnachie-Landshoff form-factor[29]. It is found that the \mathcal{P} omeron Regge trajectory requires a quadratic term such that, $\alpha(t) = 1.10 + 0.25t + \alpha''t^2$, with $\alpha'' = 0.079 \pm 0.012$ GeV⁻⁴. The factor, e^{bt} , compensates for the effect that the quadratic term has on the normalization⁴. s' has units of GeV².

It has been found in Ref. [12] that a $\sigma_{\mathcal{P}p}^{total}$ with only one term is inadequate to understand the existing single diffractive data. Thus, in analogy with all total hadronic cross sections[30], $\sigma_{\mathcal{P}p}^{total}$ is written with two components. The first term is due to \mathcal{P} omeron-exchange and dominates at large s' . The second term is due to C=+1 (a/f_2) Reggeon exchange and dominates at small s' . The exponents in the two terms of $\sigma_{\mathcal{P}p}^{total}$ are from Refs. [31, 32]. R is a free parameter in the fits. It may be noted that Eq. 8 is equivalent to the \mathcal{P} omeron- \mathcal{P} omeron- \mathcal{P} omeron and \mathcal{P} omeron- \mathcal{P} omeron-Reggeon terms in a triple-Regge expansion (see, for example, Ref. [25]).

Table 2 shows the results[12] for two of the various fits of Eq. 8 to the data. Fit “A” was made in the low-background region, $0.03 < \xi < 0.04$, and the small residual background ($\sim 15\%$) was ignored. Fit “A” is plotted in Fig. 4 superimposed on the data in that ξ -bin and is seen to describe the data quite well. Fit “D” is made to data in the larger range $0.03 < \xi < 0.09$, with a conventional background term[33], $A\xi^1 e^{ct}$, added to Eq. 8, where A and c are different for the ISR data and the UA8 data. The two types of fits are self-consistent.

There are several noteworthy results. First, we find:

$$K\sigma_0 = 0.72 \pm 0.10 \text{ mb GeV}^{-2}$$

which, if factorization is valid, provides a normalization to all diffractive processes. Second, the value found for R (4.0 ± 0.6) is close to that found in the fits to pp and $p\bar{p}$ total cross sections[32, 31], illustrating that the relative strengths of \mathcal{P} omeron-exchange and a/f_2 exchange in \mathcal{P} omeron-proton scattering are similar to that found in pp scattering.

We note that there is an implicit systematic uncertainty in the above value of $K\sigma_0$ due to the choice of exponents of $\sigma_{\mathcal{P}p}^{total}$ in Eq. 8 (see Refs. [30, 31, 32]). However, as discussed below, this particular uncertainty cancels out when the product of $K\sigma_0$ and f/σ_0 is taken.

⁴Donnachie & Landshoff[29] suggest that $\sigma_{\mathcal{P}p}^{total}$ may also depend on momentum transfer, t . We ignore that possibility in this paper, but note that any such dependence may be absorbed in this e^{bt} factor.

4 Results

We now use the techniques of the previous section to determine fK and the absolute cross section for jet production in React. 1. The solid points in Fig. 5(a) are the experimental \mathcal{R} ratios from Table 1, before corrections for non- \mathcal{P} omeron-exchange background. To correct \mathcal{R} for the background in its denominator, we divide it by the fraction of the single diffractive signal which is \mathcal{P} omeron-exchange[12], $\frac{s}{s+b}$, given in Table 3. The results are plotted as the open points in Fig. 5. We discuss below the possible contribution of background to the numerator.

Table 3 contains the fitted single diffraction cross section[12], $\frac{d^2\sigma}{d\xi dt}$, which has been integrated over t from 1.15-2.0 GeV², $\frac{d\sigma_{sd}}{d\xi}$. This quantity is multiplied by the \mathcal{R} ratios in Table 1 to find the absolute jet cross sections given in Table 3. $\frac{d\sigma_{sd}}{d\xi}$ and the background contribution to single diffraction, b , are plotted in Fig. 5(b).

A prediction for the s' -dependence of the \mathcal{R} ratio in Fig. 5(a) can be made using Eq. 7, with $\sigma_{\mathcal{P}p}^{total}$ replaced by the two-component version shown in Eq. 8. The solid curve in Fig. 5(a) shows this quantity:

$$\mathcal{R}(s') = \frac{\sigma_{\mathcal{P}p}^{jets}(s')}{(s')^{0.10} + 4(s')^{-0.32}} \cdot \frac{f}{\sigma_0} \quad (9)$$

normalized to the two open points at largest x_p , where the background corrections are smallest. This yields a fitted f/σ_0 value of $0.532 \pm 0.081(\text{stat}) \pm 0.160(\text{sys}) \text{ mb}^{-1}$. The uncertainty from the choice of the exponents used is the same as mentioned above for the determination of $K\sigma_0$, but now appears in the denominator, so that there is a cancellation when the product is taken to arrive at the final fK values.

At this point, we note that background in the numerator of \mathcal{R} , jet events from $(q\bar{q})$ Reggeon exchange, has been neglected. The fact that the two open points at smaller x_p in Fig. 5 do not lie above the fitted solid curve signifies that such non- \mathcal{P} omeron-exchange background is insignificant in the numerator. This may be understood by noting that the calculated $(q\bar{q})$ jet cross sections in Table 1 are a factor 2.3 times smaller than their gluonic counterparts. Furthermore, the Reggeon flux factor is likely to be smaller than $F_{\mathcal{P}/p}(t, \xi)$.

Based on this argument, an improved determination of f/σ_0 should be possible by fitting Eq. 9 to all four open points in Fig. 5. This fit is shown as the dashed curve in the figure and yields:

$$\begin{aligned} f/\sigma_0 &= 0.422 \pm 0.039(\text{stat}) \pm 0.127(\text{sys}) \text{ mb}^{-1} && \text{gluonic-}\mathcal{P}\text{omeron,} \\ f/\sigma_0 &= 0.784 \pm 0.072(\text{stat}) \pm 0.235(\text{sys}) \text{ mb}^{-1} && q\bar{q}\text{-}\mathcal{P}\text{omeron.} \end{aligned}$$

These values are only about one statistical standard deviation lower than those obtained from fitting to the two points with largest x_p .

Multiplying these values of f/σ_0 by the above value, $K\sigma_0 = 0.72$, yields:

$$\begin{aligned} fK &= 0.304 \pm 0.050(\text{stat}) \pm 0.091(\text{sys}) \text{ GeV}^{-2} && \text{gluonic-}\mathcal{P}\text{omeron,} \\ fK &= 0.564 \pm 0.094(\text{stat}) \pm 0.169(\text{sys}) \text{ GeV}^{-2} && q\bar{q}\text{-}\mathcal{P}\text{omeron.} \end{aligned}$$

With a dominant (80–90%) gluonic component in the \mathcal{P} omeron reported by the H1 Collaboration[7], our gluonic value of fK (0.30 ± 0.10) can be compared with corresponding (jet cross section) measurements of fK reported by ZEUS[5] (0.37 ± 0.15) and CDF[10] (0.11 ± 0.02).

If the \mathcal{P} omeron were like a real particle, the Donnachie-Landshoff value, $K = 0.78 \text{ GeV}^{-2}$, is thought to be “the only reasonable normalization of the Flux-Factor” [34] and the momentum sum rule might be true ($f = 1.0$). We find however that, if K has this value, $f = 0.39$ for a gluonic- \mathcal{P} omeron, while for a $q\bar{q}$ - \mathcal{P} omeron, $f = 0.72$.

With our determinations of fK and $F_{\mathcal{P}/p}(t, \xi)$, hard diffraction cross section predictions may be calculated for Reacts. 1 and 2. It is interesting to note that the curve in Fig. 5(a) is a prediction for the measured ratio, $\mathcal{R}(s')$, at any s -value in React. 1, providing the $\sqrt{s'}$ -scale is used, and background is taken into account. Comparisons of these predictions with data samples from other experiments will test the basic assumption of factorization used in our analysis.

Not discussed in this Letter is the issue of saturation of $F_{\mathcal{P}/p}(t, \xi)$ at high energies, which Goulianos[15] points out is required if the triple-Regge prediction of σ_{sd}^{total} is to agree with experiment and not violate unitarity. We mention this here because Ref. [15] proposes that saturation be achieved by having K decrease with increasing energy, s . However, Ref. [12] shows that the observed s -dependence of $\frac{d^2\sigma}{d\xi dt}$ at fixed ξ and t is inconsistent with such an s -dependent K , but is in good agreement with a constant (i.e. s -independent) K and a $\sigma_{\mathcal{P}p}^{total}$ with 2-components, as discussed above. An alternate solution to the saturation of $F_{\mathcal{P}/p}(t, \xi)$ at high energies has been proposed[35], in which K is s -independent and $F_{\mathcal{P}/p}(t, \xi)$ is damped at small values of ξ and t .

Acknowledgements

We remain grateful to the UA2 collaboration, without whose cooperation these measurements would not have been possible, and to the CERN administration for their support. We particularly wish to thank Sandy Donnachie for his strong early support of this experiment. We are indebted to John Collins, Gunnar Ingelman, and Peter Landshoff for helpful discussions.

References

- [1] G. Ingelman and P. Schlein, Phys. Lett. B 152 (1985) 256.
- [2] For reviews, see e.g.:
K. Goulianos, Phys. Rep. 101 (1983) 169;
G. Alberi and G. Goggi, Phys. Rep. 74 (1981) 1;
A.B. Kaidalov, Phys. Rep. 50 (1979) 157;
U. Amaldi, M. Jacob and G. Matthiae, Ann. Rev. Nucl. Sci. 26 (1976) 385.
- [3] R. Bonino et al. [UA8 Collaboration], Phys. Lett. B 211 (1988) 239.
- [4] A. Brandt et al. [UA8 Collaboration], Phys. Lett. B 297 (1992) 417.
- [5] M. Derrick et al. [ZEUS Collaboration], Phys. Lett. B 315 (1993) 481; 332 (1994) 228; 338 (1994) 483; 356 (1995) 129; Zeit. Phys. C 68 (1995) 569.
- [6] T. Ahmed et al. [H1 Collaboration], Nucl. Phys. B 429 (1994) 477; Phys. Lett. B 348 (1995) 681.
- [7] C. Adloff et al. [H1 Collaboration], Z. Phys. C76 (1997) 613.
- [8] A. Brandt [DØ Collaboration], Proceedings of the 11th Topical Workshop on Proton-Antiproton Collider Physics, Abano Terme, Italy (1996).
- [9] F. Abe et al. [CDF Collaboration], Phys. Rev. Letters 78 (1997) 2698.
- [10] F. Abe et al. [CDF Collaboration], Phys. Rev. Letters 79 (1997) 2636.
- [11] P. Schlein [UA8 Collaboration], “The Evidence for Partonic Behavior of the Pomeron”, Proceedings of the International Europhysics Conference on High Energy Physics - Marseille, France, 22-28 July 1993 (Editions Frontieres - ed. J. Carr and M Perrottet) p. 592.
- [12] A. Brandt et al. [UA8 Collaboration], “Measurements of Single Diffraction at $\sqrt{s} = 630$ GeV; Evidence for a Non-Linear $\alpha(t)$ of the \mathcal{P} omeron”, Nucl. Phys. B, (in press - 1998) – also hep-ex/9719004.
- [13] A. Donnachie and P.V. Landshoff, Nucl. Phys. B 303 (1988) 634.
- [14] E.L. Berger, J.C. Collins, D.E. Soper, G. Sterman, Nucl. Phys. B 286 (1987) 704.
- [15] K. Goulianos, Phys. Letters B 358 (1995) 379; B 363 (1995) 268.
- [16] A. Brandt et al. [UA8 Collaboration], Nucl. Instrum. & Methods A 327 (1993) 412.

- [17] A. Beer et al. [UA2 Collaboration], Nucl. Instrum. & Methods A 224 (1984) 360; C. N. Booth, Proceedings of the 6th Topical Workshop on Proton-Antiproton Collider Physics - Aachen 1986, (World Scientific, Singapore, 1987; eds. K. Eggert et al.) p. 381.
- [18] J.G. Zweizig et al., Nucl. Instrum. & Methods A 263 (1988) 188.
- [19] A. Brandt, Ph.D. Thesis, University of California, Los Angeles (1992).
- [20] H.-U. Bengtsson, G. Ingelman, Comput. Phys. Commun. 34 (1985) 251; H.-U. Bengtsson, T. Sjostrand, Comput. Phys. Commun. 46 (1987) 43.
- [21] G. Ingelman, "Monte Carlo for Diffractive Hard Scattering", a precursor to POMPYT: P. Bruni and G. Ingelman, DESY 93-187; Proceedings of the International Europhysics Conference on High Energy Physics - Marseille, France, 22-28 July 1993 (Editions Frontieres - ed. J. Carr and M Perrottet) p. 595.
See also the POMPYT Homepage: <http://www3.tsl.uu.se/thepp/pompyt/>
- [22] T. Sjostrand, Comput. Phys. Commun. 39 (1986) 347; T. Sjostrand and M. Bengtsson, Comput. Phys. Commun. 43 (1987) 367.
- [23] B. Andersson, G. Gustafson, G. Ingelman & T. Sjostrand, Phys. Rep. 97 (1983) 31.
- [24] J. Alitti et al. [UA2 Collaboration], Phys. Lett. B 257 (1991) 232; see also UA2 $p\bar{p}$ Note 580.
- [25] R.D. Field & G. Fox, Nucl. Phys. B 80 (1974) 367.
- [26] see: A.B. Kaidalov, in Ref. 2.
- [27] R.L. Cool et al., Phys. Rev. Lett. 47 (1981) 701.
- [28] M.G. Albrow et al., Nucl. Phys B 72 (1974) 376; M.G. Albrow et al., Nucl. Phys B 54 (1973) 6.
- [29] A. Donnachie and P.V. Landshoff, Nucl. Phys. B 244 (1984) 322; A. Donnachie and P.V. Landshoff, Nucl. Phys. B 231 (1984) 189.
- [30] A. Donnachie and P.V. Landshoff, Phys. Letters B 296 (1992) 227.
- [31] R.J.M. Covolan, J. Montanha and K. Goulianos, Phys. Letters B 389 (1996) 176.
- [32] J.-R. Cudell, K. Kang and S.K. Kim, preprint Brown-HET-1060, January 1997.
- [33] For example, see: J.C. Sens, Proceedings of 14th Scottish Universities Summer School in Physics (Academic Press - 1974; eds. R.L. Crawford & R. Jennings) 105; M.G. Albrow et al., Nucl. Phys. B 108 (1976) 1, and references therein.
- [34] P. Landshoff, private communication (1997).

- [35] S. Erhan and P. Schlein, presented at 3rd Workshop on Small- x and Diffractive Physics (Argonne - Sept. 1996), and DIS97 conference (Chicago - April 1997), Proceedings to be published.

ξ	$\sqrt{s'}$ GeV	N_j	gluonic – Pomeron		q \bar{q} – Pomeron	
			$\mathcal{R} = \frac{\Delta\sigma_{sd}^{jets}}{\Delta\sigma_{sd}^{total}}$	$\sigma_{\mathcal{P}p}^{jets}$	$\mathcal{R} = \frac{\Delta\sigma_{sd}^{jets}}{\Delta\sigma_{sd}^{total}}$	$\sigma_{\mathcal{P}p}^{jets}$
			$\times 10^{-3}$	mb	$\times 10^{-3}$	mb
.03-.04	118	11	2.1 ± 0.6	0.0149	1.8 ± 0.5	0.0064
.04-.06	140	35	2.8 ± 0.5	0.0209	2.3 ± 0.4	0.0090
.06-.08	167	25	1.7 ± 0.3	0.0282	1.4 ± 0.3	0.0121
.08-.10	189	39	2.7 ± 0.4	0.0353	2.3 ± 0.3	0.0149

Table 1: Numbers of 2-jet events, cross section ratios corrected to scattered partons with $p_T > 8$ GeV, as explained in the text, and calculated values of $\sigma_{\mathcal{P}p}^{jets}$ for the same conditions. The ratios are for data in the momentum-transfer range, 1.15-2.0 GeV².

ξ -range		Fit “A” 0.03-0.04	Fit “D” 0.03-0.09
χ^2		65	393
No. of Data points		48	292
$\chi^2/\text{degree of freedom}$		1.5	1.4
$K\sigma_0$	mb GeV ⁻²	0.67 ± 0.08	0.72 ± 0.10
α''	GeV ⁻⁴	0.078 ± 0.013	0.079 ± 0.012
b	GeV ⁻²	0.88 ± 0.19	1.08 ± 0.20
R		5.0 ± 0.6	4.0 ± 0.6
$A(\text{UA8})$	mb GeV ⁻²	–	25 ± 7
$A(551)$	mb GeV ⁻²	–	280 ± 30
$A(930)$	mb GeV ⁻²	–	226 ± 21
$c(\text{UA8})$	GeV ⁻²	–	2.1 ± 0.2
$c(\text{ISR})$	GeV ⁻²	–	3.5 ± 0.1

Table 2: Fit results[12] of Eq. 8 to experimental values of $d^2\sigma/d\xi dt$ (mb/GeV²) from UA8 and ISR[28]. Fit “A” includes no background; Fit “D” includes background of the form $A\xi^1 e^{ct}$, A and c are different for UA8 and ISR data. The bottom part of the table includes the fitted parameters of the background.

ξ	$\sqrt{s'}$ GeV	$\frac{d\sigma_{sd}}{d\xi}$ mb	$\frac{s}{s+b}$	$\frac{d\sigma_{jets}}{d\xi}$ μb
.03-.04	118	0.159	0.81	0.33 ± 0.10
.04-.06	140	0.142	0.69	0.40 ± 0.07
.06-.08	167	0.139	0.55	0.24 ± 0.04
.08-.10	189	0.143	0.45	0.39 ± 0.06

Table 3: Single-diffractive (single arm) differential cross sections[12] integrated over the momentum transfer range, $t = 1.15\text{-}2.0 \text{ GeV}^2$. Column 4 shows the fraction[12] of the the single-diffractive cross section which is \mathcal{P} omeron-exchange. The di-jet differential cross sections in Column 5, for the same t -range, are obtained by multiplying Column 3 by the \mathcal{R} values for the gluonic- \mathcal{P} omeron in Table 1. There is a 30% systematic uncertainty on the jet cross sections.

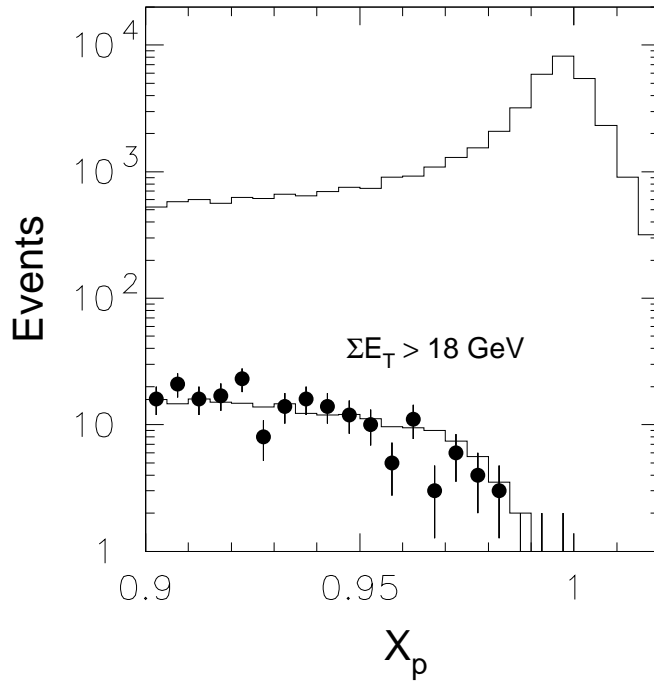


Figure 1: The upper histogram shows the observed dependence of event yield on proton momentum fraction, x_p , for “DIF” trigger events (inclusive protons or antiprotons). The solid points are those “DIF” trigger events that have $\Sigma E_T > 18$ GeV (offline evaluation); The lower histogram, which is normalized to the solid points, corresponds to the high-statistics sample for which the same ΣE_T selection was imposed online in the “JET” trigger.

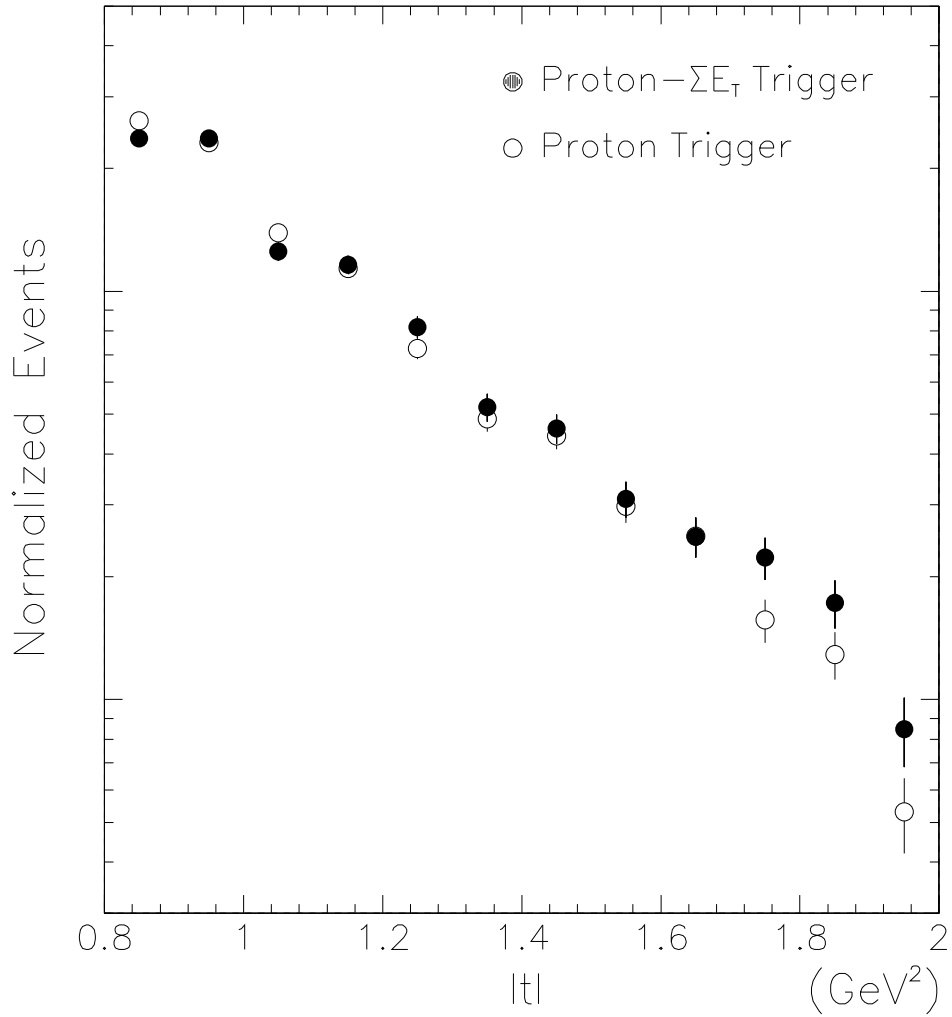


Figure 2: Momentum transfer (t) dependence of the raw data samples for both “DIF” (inclusive-proton) and “JET” (proton- ΣE_T) triggers, when $0.90 < x_p < 0.97$ and after (offline) rejection of pileup and halo background[19]. The two distributions are normalized to one another with an arbitrary scale.

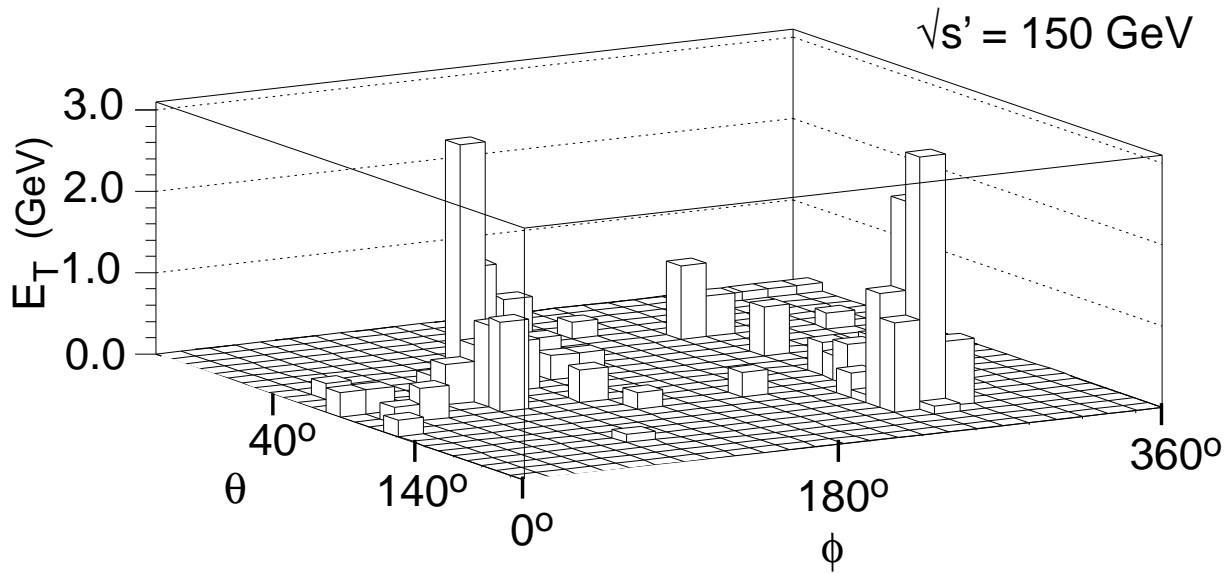


Figure 3: A typical raw UA8 2-jet event display in the UA2 calorimeter: cell energies in a θ vs. ϕ projection (the complete event is shown). Each jet has $E_T^{jet} > 8 \text{ GeV}$. The proton in this event had a measured $x_p = 0.94$.

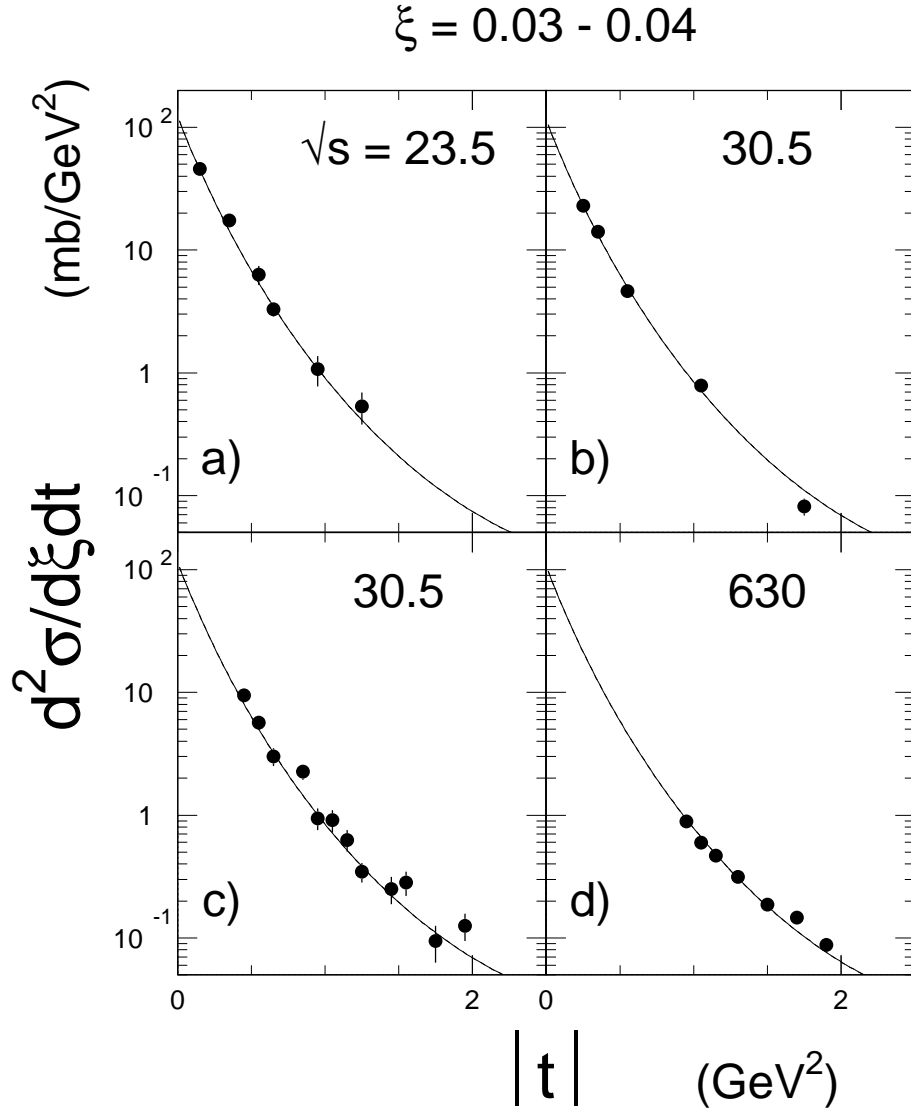


Figure 4: Differential cross section, $\frac{d^2\sigma}{d\xi dt}$, vs t , for three ISR measurements[28] and UA8[12]. Points are averages of data in the ξ -range 0.03–0.04. The curves correspond to Fit “A” in Table 2 evaluated at $\xi = 0.035$. It is shown in Ref. [12] that the relative normalizations of these data sets directly reflect the s' -dependence of σ_{pp}^{total} .

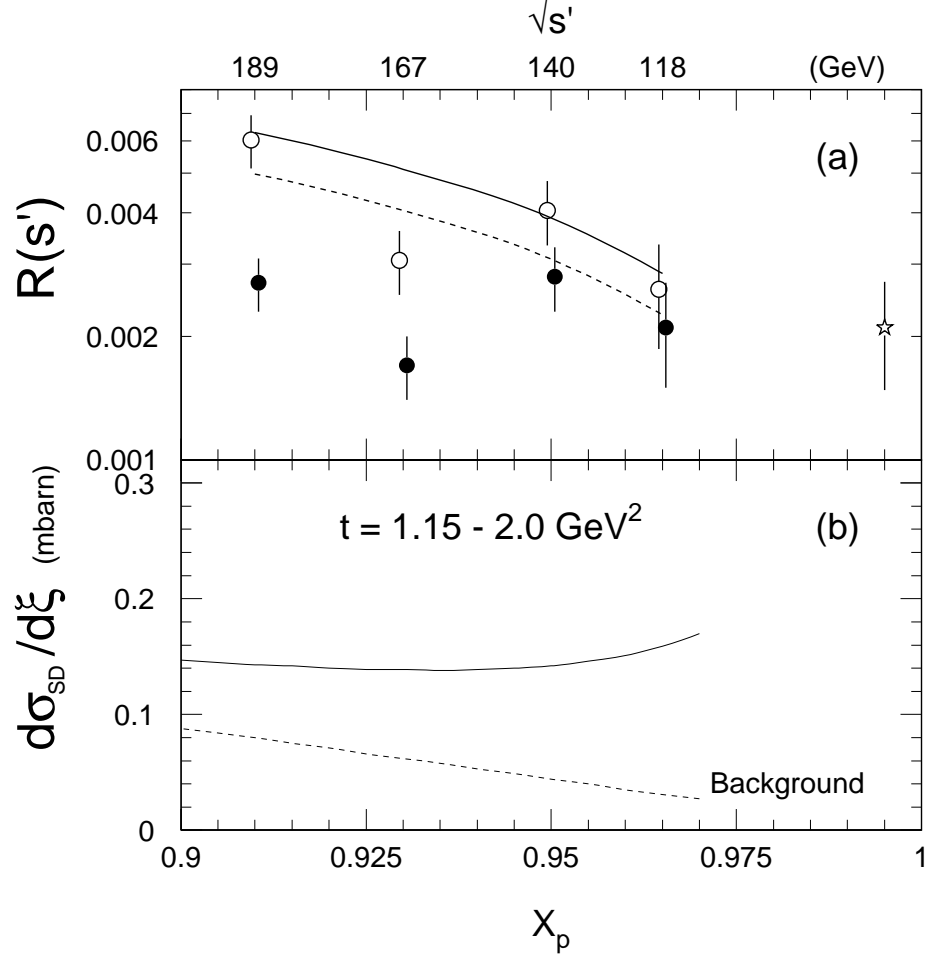


Figure 5: (a) Measured cross-section ratio, \mathcal{R} (solid points) for a hard gluonic \mathcal{P} omeron, vs. proton momentum fraction and diffractive mass. The star point on the right-hand-side shows the systematic uncertainty. As explained in the text, the open points contain a correction for non- \mathcal{P} omeron-exchange background in the denominator of \mathcal{R} . The solid curve, normalized to the two right-hand points, is a prediction discussed in the text. The dashed curve is the same, but normalized to all four open points; (b) Solid curve is a fit to the measured differential cross section[12], $d\sigma_{sd}/d\xi$, for inclusive single diffraction. The dashed curve is the fitted non- \mathcal{P} omeron-exchange background in the observed cross section.